Symposium on Applied Aerodynamics and Design of Aerospace Vehicle (SAROD 2013)
November 21-23, 2013, Hyderabad, India

Dynamic Modeling of Medium Size Aerostat with Tether

A Sharma[1], A Kumar[2], P Gupta[3], A Pal[4], S C Sati[5], A K Ghosh[6]
Aerial Delivery Research & Development Establishment (ADRDE), DRDO, Agra, India
(adrde.aeg@gmail.com)

ABSTRACT

An Aerostat is a lighter than air tethered platform which is primarily used for surveillance. However, the Dynamic Analysis of the Aerostat with Tether is very important considering the response of the complete system to various wind disturbances. This analysis is also used for payload stability requirement generation. This research work presents an analysis to determine the dynamic response behavior of the Aerostat with tether due to wind disturbances. 6-DOF modeling of aerostat is presented. Dynamic Modeling of Tether is carried out using an efficient recursive rigid body dynamics approach. Modeling for aerostat balloon and tether are then clubbed to model the dynamic behavior of complete system. Results are presented for the dynamic response behavior of aerostat with tether to various wind disturbances and it is observed that the system is dynamically stable to the wind loadings considered.

Key Words: Dynamic Modeling, 6-DOF, Aerostat, Tether

1. INTRODUCTION

Conventional tethered aerostats are used to provide high-resolution imagery to ground installations, as well as to provide communications and data-relay to wide areas over any terrain. Unlike fixed-wing aircraft or helicopters, aerostats are lighter-than-air and are tethered to the ground by a cable that also provides power.

Aerostats have the potential to be used in a variety of areas such as low and moderate altitude applications. They can also be used as heavy-lift vehicles and could possibly be a solution for near-space missions. Thus, interest in the modeling and analysis of aerostat dynamics has been growing.

2. OVERVIEW OF THE WORK DONE

There are several ways to model aerostat dynamics. In all cases, the aerostat has a similar model that includes aerodynamics, buoyancy and apparent mass whereas significantly different approaches are taken in modeling the tether. Although the tether is continuous, it is often modeled using discrete elements.

The simplest aerostat-tether models use lumped-mass bodies connected with elastic elements where each mass has only 3 Degrees-Of-Freedom (DOF). A limitation of the simple lumped-mass model is that for stiff tethers, the elastic elements must also be stiff to mimic low strain, resulting in potentially high-frequency vibrations.

Another approach to tether modeling is using beam elements rather than lumped masses. Using beam elements allows modeling of bending moments but requires a finite element non-linear solver.

Tethered aerostats typically result in low tension in the tethers limited by the buoyancy. Strength of the tether is usually sufficient so that limitations in strain on fibre optics are not exceeded, resulting in the tether strain being small compared with the tether sway and surge.

In this research work, tethers with negligible strain have been modeled using a chain of links connected by spherical joints, rather than using stiff elastic elements and lumped masses. The resulting model takes the form of an open chain common to multi-body dynamics.

This research work takes an approach similar to the joint-coordinate method where dynamics of each link is represented by a relative joint velocity, resulting in a set of unconstrained differential equations representing the tether.

3. 6-DOF DYNAMIC MODELING OF AEROSTAT

The aerostat is modeled as a rigid 6-DOF body with an attached body frame. Figure 1 represents an aerostat with tether.

A. Aerostat Forces and Moments

The various forces and moments acting on the aerostat are as follows:

[1]Scientist C, ADRDE, DRDO, Agra
[2]Scientist D, ADRDE, DRDO, Agra
[3]Scientist D, ADRDE, DRDO, Agra
[4]Scientist F, ADRDE, DRDO, Agra
[5]Director, ADRDE, DRDO, Agra
[6]Professor, Dept of Aerospace Engineering, IIT Kanpur

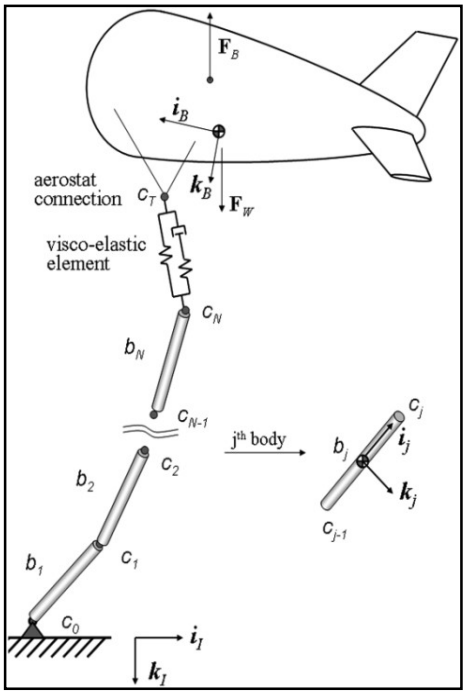

Figure 1: Aerostat with Tether

Weight and buoyancy forces: both are expressed in the inertial frame.

$$\mathbf{F}_W = \begin{Bmatrix} 0 \\ 0 \\ m_B g \end{Bmatrix}$$

$$\mathbf{F}_B = \begin{Bmatrix} 0 \\ 0 \\ -\mathrm{Vol}(\rho_a - \rho_g)g \end{Bmatrix}$$

where; m_B : aerostat mass excluding the enclosed-gas volume.

Aerodynamic forces and moments: expressed in the Aerostat body frame

$$\mathbf{F}_A = \bar{q}\mathrm{Vol}^{2/3}\mathbf{T}(\alpha)\begin{Bmatrix} -(C_{D0} + C_{D_\alpha}\alpha + C_{D_{\alpha^2}}\alpha^2) \\ C_{Y\beta}\beta + (\bar{l}/(2V_A))(C_{Yp}p + C_{Yr}r) \\ -(C_{L0} + C_{L_\alpha}\alpha + C_{L_{\alpha^2}}\alpha^2 + (\bar{l}/(2V_A))(C_{Lq}q) \end{Bmatrix}$$

$$\mathbf{M}_A = \bar{q}\mathrm{Vol}^{2/3}\bar{l}\begin{Bmatrix} C_{l\beta}\beta + (\bar{l}/(2V_A))(C_{lp}p + C_{lr}r) \\ C_{m0} + C_{m\alpha}\alpha + (\bar{l}/(2V_A))C_{mq}q \\ C_{n\beta}\beta + (\bar{l}/(2V_A))(C_{nr}r + C_{np}p) \end{Bmatrix}$$

$$\mathbf{T}(\alpha) = \begin{bmatrix} \cos\alpha & 0 & -\sin\alpha \\ 0 & 1 & 0 \\ \sin\alpha & 0 & \cos\alpha \end{bmatrix}$$

$\bar{q}$ is the dynamic pressure, the characteristic length $\bar{l}$=Vol$^{1/3}$, V_A is the aerodynamic velocity magnitude and $\mathbf{T}(\alpha)$ is the transformation matrix from relative wind frame to the body frame.

The aerodynamic velocity $\mathbf{V}_A = \{u_A\ v_A\ w_A\}^T$ is the difference of the aerostat body frame velocity and the wind velocity (expressed in the body frame),

$$\begin{Bmatrix} u_A \\ v_A \\ w_A \end{Bmatrix} = \begin{Bmatrix} u \\ v \\ w \end{Bmatrix} - \begin{Bmatrix} u_{wind} \\ v_{wind} \\ w_{wind} \end{Bmatrix}$$

The resulting aerodynamic angles are:

$$\alpha = \tan^{-1} {}^{w_A}/_{u_A}\ ;\ \beta = \sin^{-1} {}^{v_A}/_{V_A}$$

B. Apparent Mass

Vehicles which displace a large mass of fluid compared with its own mass (such as aerostats), experience additional forces and moments due to the fluid's acceleration.

Force and Moment due to apparent mass and apparent inertia

$$\mathbf{F}_{\mathrm{AM}} = -\mathbf{I}_{\mathrm{AM}}\begin{Bmatrix} \dot{u}_A \\ \dot{v}_A \\ \dot{w}_A \end{Bmatrix} - \mathbf{S}(\boldsymbol{\omega}_B)\mathbf{I}_{\mathrm{AM}}\begin{Bmatrix} u_A \\ v_A \\ w_A \end{Bmatrix}$$

$$\mathbf{M}_{\mathrm{AM}} = -\mathbf{I}_{\mathrm{AI}}\begin{Bmatrix} \dot{p}_B \\ \dot{q}_B \\ \dot{r}_B \end{Bmatrix} - \mathbf{S}(\boldsymbol{\omega}_B)\mathbf{I}_{\mathrm{AI}}\begin{Bmatrix} p_B \\ q_B \\ r_B \end{Bmatrix}$$

Where, $\mathbf{I}_{\mathrm{AM}}$ and $\mathbf{I}_{\mathrm{AI}}$ are the apparent mass and inertia matrices

$$\text{Also } \mathbf{S}(\boldsymbol{\omega}_B) = \begin{bmatrix} 0 & -r_B & q_B \\ r_B & 0 & -p_B \\ -q_B & p_B & 0 \end{bmatrix}$$

$$\boldsymbol{\omega}_B = \begin{Bmatrix} p_B \\ q_B \\ r_B \end{Bmatrix}$$

The above equation when expressed in terms of the aerostat body velocities and inertial winds w_x, w_y and w_z is as follows:

$$\mathbf{F}_{\mathrm{AM}} = -\mathbf{I}_{\mathrm{AM}}\left(\begin{Bmatrix} \dot{u} \\ \dot{v} \\ \dot{w} \end{Bmatrix} - \mathbf{T}_I^B\begin{Bmatrix} \dot{w}_x \\ \dot{w}_y \\ \dot{w}_z \end{Bmatrix}\right) + (\mathbf{S}(\boldsymbol{\omega}_B)\mathbf{I}_{\mathrm{AM}} - \mathbf{I}_{\mathrm{AM}}\mathbf{S}(\boldsymbol{\omega}_B))\mathbf{T}_I^B\begin{Bmatrix} w_x \\ w_y \\ w_z \end{Bmatrix} - \mathbf{S}(\boldsymbol{\omega}_B)\mathbf{I}_{\mathrm{AM}}\begin{Bmatrix} u \\ v \\ w \end{Bmatrix}$$

C. Visco-elastic Link

The visco-elastic element connecting the aerostat and tether is composed of a spring with static stiffness K_s in parallel with a viscous spring of stiffness K_v and viscous damper with damping coefficient C_v.

Visco-elastic line force is written in terms of components Δx, Δy, and Δz of the difference vector formed by subtracting the inertial position of the aerostat connection C_P and the tether connection C_N.

$$\mathbf{F}_T = \frac{F_T}{s_{ve}}\begin{Bmatrix}\Delta x\\ \Delta \mathrm{y}\\ \Delta \mathrm{z}\end{Bmatrix}$$

Where, $S_{ve} = \sqrt{\Delta x^2 + \Delta y^2 + \Delta z^2}$ is the stretch and the stretch rate is $\dot{S_{ve}}$.

The differential equation for the Visco-elastic internal force $\mathbf{F}_T$ in terms of the stretch, stretch rate and L_{ve}, the unstretched length is as follows:

$$\dot{F}_T + \frac{K_v}{C_v}F_T = \begin{cases}(K_v + K_s)\dot{s}_{ve} + \dfrac{K_v K_s}{C_v}(s_{ve} - L_{ve}), & s_{ve} - L_{ve} > 0\\ 0 & s_{ve} - L_{ve} \le 0\end{cases}$$

The first condition represents the Visco-elastic element in tension, and the second represents the slack case, in which the internal force decays to zero.

D. Aerostat Dynamic Equations

Equating the sum of external forces to the time derivative of linear momentum and equating the sum of moments about the aerostat mass center to the time derivative of angular momentum, gives the following:

$$\begin{aligned}\Big(\big(m_B + m_{gas}\big)\mathbf{E}_3 + \mathbf{I}_{\mathrm{AM}}\Big)\begin{Bmatrix}\dot{u}\\ \dot{v}\\ \dot{w}\end{Bmatrix} &= \mathbf{F}_A + \mathbf{T}_I^B(\mathbf{F}_W + \mathbf{F}_B - \mathbf{F}_T)\\ &- \mathbf{S}(\boldsymbol{\omega}_B)\Big(\big(m + m_{gas}\big)\mathbf{E}_3\\ &+ \mathbf{I}_{\mathrm{AM}}\Big)\begin{Bmatrix}u\\ v\\ w\end{Bmatrix} + \mathbf{I}_{\mathrm{AM}}\mathbf{T}_I^B\begin{Bmatrix}\dot{w}_x\\ \dot{w}_y\\ \dot{w}_z\end{Bmatrix}\\ &+ \big(\mathbf{S}(\boldsymbol{\omega}_B)\mathbf{I}_{\mathrm{AM}} - \mathbf{I}_{\mathrm{AM}}\mathbf{S}(\boldsymbol{\omega}_B)\big)\mathbf{T}_I^B\begin{Bmatrix}w_x\\ w_y\\ w_z\end{Bmatrix}\end{aligned}$$

And $$(\mathbf{I}_B + \mathbf{I}_{\mathrm{AI}})\begin{Bmatrix}\dot{p}_B\\ \dot{q}_B\\ \dot{r}_B\end{Bmatrix} = \mathbf{M}_A + \mathbf{S}\big(\mathbf{r}_{cg}^{cb}\big)\mathbf{T}_I^B\mathbf{F}_B - \mathbf{S}\big(\mathbf{r}_{cg}^{cp}\big)\mathbf{T}_I^B\mathbf{F}_T - \mathbf{S}(\omega_B)(\mathbf{I}_B + \mathbf{I}_{\mathrm{AI}})\begin{Bmatrix}p_B\\ q_B\\ r_B\end{Bmatrix}$$

where $\mathbf{r}_{cg}^{cb}$ and $\mathbf{r}_{cg}^{cp}$ are the position vectors from the aerostat mass center to the center of buoyancy and aerostat connection, and $\mathbf{I}_B$ is the aerostat inertia matrix.

4. RECURSIVE DYNAMIC MODELING OF TETHER

The tether is divided into a chain of **N** bodies connected by spherical joints with each link being a body of revolution. Figure 1 shows the tether attached to the ground with the '**j**'th body, $\boldsymbol{b}_j$, having two connections, joints c_{j-1} and c_j , and an external load applied to the *N*th body. The *N*th body, b_N, is the terminal link, body b_1 is the root link, and b_0 is a fixed body or ground where connection c_0 is stationary. A body, b_j, is attached to its parent, $b_{j\mathrm{p}}$, in the direction of the ground where the subscript 'j_{p}' represents the parent of 'j' . Body b_0 is attached to a fixed or inertial frame (*I*) defined by three orthogonal unit vectors $\mathbf{i}_I$, $\mathbf{j}_I$, and $\mathbf{k}_I$.

A body reference frame is assigned to each link with the origin at the link's mass centre and the vector $\mathbf{i}_j$ collinear to the mass centre and joints on body j with $\mathbf{j}_j$ and $\mathbf{k}_j$ defined to form an orthogonal triad.

In the tether model, the configuration has spherical joints connecting the N slender bodies with no applied twisting torque at the ground or terminal link. The combination results in the spin dynamics of each body having a minimal affect on the tether's overall motion. Thus, the tether spin can be eliminated and it aids in efficient computation of recursive dynamics.

Angular velocity of the j[th] body in the inertial frame is

$$\boldsymbol{\omega}_{j/I} = q_j\mathbf{j}_j + r_j\mathbf{k}_j$$

$\boldsymbol{\omega}_{j/I}$ expressed as the sum of the previous body's angular velocity and the relative angular velocity of the j[th] link and its preceding link $\boldsymbol{\omega}_{j/j-1}$:

$$\boldsymbol{\omega}_{j/I} = \boldsymbol{\omega}_{j/j-1} + \mathbf{T}_{j-1}^j\boldsymbol{\omega}_{j-1/I}$$

$$\boldsymbol{\omega}_{j/I} = \begin{Bmatrix}\omega_{xj}\\ \omega_{yj}\\ \omega_{zj}\end{Bmatrix} + \mathbf{T}_{j-1}^j\begin{Bmatrix}0\\ q_{j-1}\\ r_{j-1}\end{Bmatrix} = \begin{Bmatrix}0\\ q_j\\ r_j\end{Bmatrix}$$

Simplifying the above equation: The first row is not considered in further formulations

$$\omega_{xj} = -\tilde{\mathbf{T}}_{j-1}^j\begin{Bmatrix}q_{j-1}\\ r_{j-1}\end{Bmatrix}$$

$$\tilde{\boldsymbol{\omega}}_{j/I} = \begin{Bmatrix}\omega_{yj}\\ \omega_{zj}\end{Bmatrix} + \hat{\mathbf{T}}_{j-1}^j\begin{Bmatrix}q_{j-1}\\ r_{j-1}\end{Bmatrix} = \begin{Bmatrix}q_j\\ r_j\end{Bmatrix}$$

Where, $\tilde{\mathbf{T}}_{j-1}^j$1 is a 1 x 2 sub matrix formed from the second and third elements of the first row of $\mathbf{T}_{j-1}^j$, and $\hat{\mathbf{T}}_{j-1}^j$ is a 2 x 2 sub matrix formed from the

second and third columns of the second and third rows of $\mathbf{T}_{j-1}^{j}$.

For the ground link both q_o and r_o are zero. Thus for the root link

$$\omega_{x1} = 0$$

$$\tilde{\boldsymbol{\omega}}_{1/I} = \begin{Bmatrix} \omega_{y1} \\ \omega_{z1} \end{Bmatrix} = \begin{Bmatrix} q_1 \\ r_1 \end{Bmatrix}$$

Differentiation of the angular velocity with respect to the inertial frame results in the angular acceleration of the j^{th} body taking the recursive form

$$\boldsymbol{\alpha}_{j/I} = \dot{\boldsymbol{\omega}}_{j/(j-1)} + \boldsymbol{\omega}_{j/I} \times \boldsymbol{\omega}_{j/j-1} + \mathbf{T}_{j-1}^{j} \boldsymbol{\alpha}_{j-1/I}$$

where $\dot{\boldsymbol{\omega}}_{j/j-1}$ is the angular acceleration of b_j with respect to b_{j-1} expressed in the b_j frame.

$$\boldsymbol{\alpha}_{j/I} = \begin{Bmatrix} 0 \\ \dot{q}_j \\ \dot{r}_j \end{Bmatrix} = \begin{Bmatrix} \dot{\omega}_{xj} \\ \dot{\omega}_{yj} \\ \dot{\omega}_{zj} \end{Bmatrix} + \begin{Bmatrix} -r_j\omega_{yj} + q_j\omega_{zj} \\ r_j\omega_{xj} \\ -q_j\omega_{xj} \end{Bmatrix} + \mathbf{T}_{j-1}^{j} \begin{Bmatrix} 0 \\ \dot{q}_{j-1} \\ \dot{r}_{j-1} \end{Bmatrix}$$

Again neglecting the first row as it is satisfied by the assumption of no twisting torque,

$$\tilde{\boldsymbol{\alpha}}_{j/I} = \begin{Bmatrix} \dot{q}_j \\ \dot{r}_j \end{Bmatrix} = \begin{Bmatrix} \dot{\omega}_{yj} \\ \dot{\omega}_{zj} \end{Bmatrix} - \begin{Bmatrix} r_j \\ -q_j \end{Bmatrix} \tilde{\mathbf{T}}_{j-1}^{j} \begin{Bmatrix} q_{j-1} \\ r_{j-1} \end{Bmatrix} + \hat{\mathbf{T}}_{j-1}^{j} \begin{Bmatrix} \dot{q}_{j-1} \\ \dot{r}_{j-1} \end{Bmatrix}$$

Compactly written as:

$$\tilde{\boldsymbol{\alpha}}_{j/I} = \dot{\boldsymbol{\omega}}_j + \boldsymbol{\lambda}_j + \hat{\mathbf{T}}_{j-1}^{j} \tilde{\boldsymbol{\alpha}}_{j-1/I}$$

Where $\boldsymbol{\lambda}_j = \begin{Bmatrix} r_j \\ -q_j \end{Bmatrix} \tilde{\mathbf{T}}_{j-1}^{j} \begin{Bmatrix} q_{j-1} \\ r_{j-1} \end{Bmatrix}$

$$\dot{\boldsymbol{\omega}}_j = \begin{Bmatrix} \dot{\omega}_{yj} & \dot{\omega}_{zj} \end{Bmatrix}^T$$

Acceleration of the j^{th} body's mass center $\mathbf{a}_j^m$ and acceleration of the jth connection joint $\mathbf{a}_j^c$ for j = 0 to N - 1, written in the b_j frame,

$$\mathbf{a}_j^m = \mathbf{T}_{j-1}^{j} \mathbf{a}_{j-1}^c + \boldsymbol{\alpha}_{j/I} \times \mathbf{r}_j^m + \boldsymbol{\omega}_{j/I} \times \left(\boldsymbol{\omega}_{j/I} \times \mathbf{r}_j^m \right)$$

$$= \mathbf{T}_{j-1}^{j} \mathbf{a}_{j-1}^c - \mathbf{r}_j^c \times \boldsymbol{\alpha}_{j/I} + \boldsymbol{\omega}_{j/I} \times \left(\boldsymbol{\omega}_{j/I} \times \mathbf{r}_j^c \right)$$

The angular acceleration components of b_j and acceleration of the (j-1)th joint equation is combined into a 5 x 1 acceleration vector; $\dot{\mathbf{v}}_j = \left\{ \tilde{\boldsymbol{\alpha}}_{j/I} \; \mathbf{a}_{j-1}^c \right\}^T$

$$\dot{\mathbf{v}}_j = \mathbf{D}_j \dot{\mathbf{v}}_{j-1} + \mathbf{G}_j \dot{\boldsymbol{\omega}}_j + \boldsymbol{\Lambda}_j$$

Where $\mathbf{D}_j = \begin{bmatrix} \hat{\mathbf{T}}_{j-1}^{j} & 0 \\ \left(\hat{\mathbf{S}}_j^c \right)^T & \mathbf{T}_{j-2}^{j-1} \end{bmatrix}, \boldsymbol{G}_j = \begin{bmatrix} \mathbf{E}_2 \\ 0 \end{bmatrix}$

$$\boldsymbol{\Lambda}_j = \begin{bmatrix} \boldsymbol{\lambda}_j \\ \boldsymbol{\omega}_{(j-1)/I} \times \left(\boldsymbol{\omega}_{(j-1)/I} \times \mathbf{r}_{j-1}^c \right) \end{bmatrix}$$

$$\hat{\mathbf{S}}_j^c = \begin{bmatrix} 0 & 0 & -x_{cj} \\ 0 & x_{cj} & 0 \end{bmatrix}$$

A. Terminal Body Recursive Dynamics

A total of 2-N vector equations are assembled, N force equations and N moment equations. Forces on each body include its weight $\mathbf{W}_j$ and an external aerodynamic force $\mathbf{F}_{Dj}$ (both defined in the inertial frame), a reaction force $-\mathbf{R}_j$ on body b_j (defined in the b_j frame) acting at the jth joint for all j except for the terminal body. An equal-but-opposite reaction $\mathbf{R}_j$ is present on body b_{j+1}.

A moment $-\mathbf{L}_j$ on body b_j (defined in the b_j frame) occurs at the j^{th} joint for all j except for the terminal body. An equal but-opposite moment $\mathbf{L}_j$ is also present on body b_{j+1}. Since the model neglects spin dynamics, the moment $\mathbf{L}_j$ cannot impart a twisting moment.

The terminal link has an external load $\mathbf{F}_T$ from the viscoelastic element applied at the end of the terminal body.

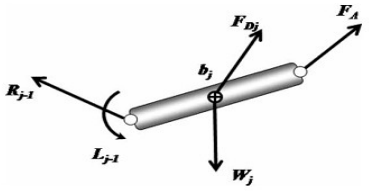

Figure 2: Terminal Link

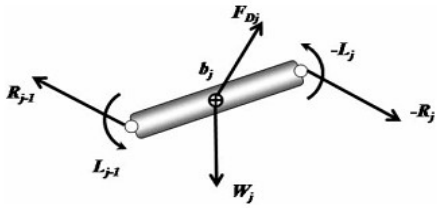

Figure 3: Non-Terminal Link

Forces acting on the terminal link (j = N), in the (j - 1)th body frame:

$$\mathbf{R}_{j-1} + \mathbf{T}_I^{j-1}(\mathbf{F}_{Dj} + \mathbf{W}_j + \mathbf{F}_T) = m_j\left(\mathbf{T}_{j-1}^{j}\right)^T \mathbf{a}_j^m$$

Similarly, summing moments about the connection joint c_{j-1} for the terminal link, in the j[th] frame:

$$\mathbf{r}_j^m \times \mathbf{T}_I^j(\mathbf{F}_{Dj} + \mathbf{W}_j) + \mathbf{r}_j^c \times \mathbf{T}_I^j\mathbf{F}_T + \mathbf{T}_{j-1}^j\mathbf{L}_{j-1} = (\mathbf{I}_j\boldsymbol{\alpha}_{j/I} + \boldsymbol{\omega}_{j/I} \times \mathbf{I}_j\boldsymbol{\omega}_{j/I}) + \mathbf{r}_j^m \times m_j\mathbf{a}_j^m$$

The 1[st] component of both sides of the moment equation reduces to zero, due to each link being a body of revolution and the fact that the position vector from connection joint j - 1 to the mass center of the terminal link is defined such that it only has an 'i' component. Incorporating both the force and moment equations, the terminal link equations are assembled into a 5 x 1 force vector F_j, arranged such that the first two equations represent the two non-zero components of the moment equation and the remaining three are components of the force.

$$\mathbf{F}_j = \mathbf{M}_j\dot{\mathbf{v}}_j + \boldsymbol{\Gamma}_T$$

Where $\mathbf{F}_j = \begin{Bmatrix} 0 \\ \mathbf{R}_{j-1} \end{Bmatrix}$

$$\mathbf{M}_j = \begin{bmatrix} \tilde{\mathbf{I}}_j - m_j\tilde{\mathbf{S}}_j^m\tilde{\mathbf{S}}_j^m & m_j\hat{\mathbf{S}}_j^m\mathbf{T}_{j-1}^j \\ m_j\left(\mathbf{T}_{j-1}^j\right)^T(\hat{\mathbf{S}}_j^m)^T & m_j\mathbf{E}_3 \end{bmatrix}$$

$$\tilde{\mathbf{I}}_j = \begin{bmatrix} I_{yy} & 0 \\ 0 & I_{zz} \end{bmatrix}$$

$$\tilde{\mathbf{S}}_j^m = \begin{bmatrix} 0 & -x_{mj} \\ x_{mj} & 0 \end{bmatrix} \qquad \hat{\mathbf{S}}_j^m = \begin{bmatrix} 0 & 0 & -x_{mj} \\ 0 & -x_{mj} & 0 \end{bmatrix}$$

$$\boldsymbol{\Gamma}_T = \begin{bmatrix} -\hat{\mathbf{S}}_j^m\mathbf{T}_I^j(\mathbf{F}_{Dj} + \mathbf{W}_j) - \hat{\mathbf{S}}_j^c\mathbf{T}_I^j\mathbf{F}_T - \hat{\mathbf{T}}_{j-1}^j\tilde{\mathbf{L}}_{j-1} \\ m_j\left(\mathbf{T}_{j-1}^j\right)^T\left(\boldsymbol{\omega}_{J/I} \times (\boldsymbol{\omega}_{J/I} \times \mathbf{r}_j^m)\right) - \mathbf{T}_I^{j-1}(\mathbf{F}_{Dj} + \mathbf{W}_j + \mathbf{F}_T) \end{bmatrix}$$

Substituting $\dot{v}_j$ gives,

$$\mathbf{F}_j = \mathbf{M}_j(\mathbf{D}_j\dot{\mathbf{v}}_{j-1} + \mathbf{G}_j\dot{\boldsymbol{\omega}}_j + \boldsymbol{\Lambda}_j) + \boldsymbol{\Gamma}_T$$

Premultiplying by $\mathbf{G}_j^T$; Note: $\mathbf{G}_j^T\mathbf{F}_j = \mathbf{0}$.

$$\dot{\boldsymbol{\omega}}_j = -(\mathbf{G}_j^T\mathbf{M}_j\mathbf{G}_j)^{-1}\mathbf{G}_j^T(\mathbf{M}_j\mathbf{D}_j\dot{\mathbf{v}}_{j-1} + \mathbf{M}_j\boldsymbol{\Lambda}_j + \boldsymbol{\Gamma}_T)$$

Substituting $\dot{\omega}_j$ and $\dot{v}_j$ in the force vector results in the final expression of F_j :

$$\mathbf{F}_j = \hat{\mathbf{M}}_j\mathbf{D}_j\dot{\mathbf{v}}_{j-1} + \hat{\boldsymbol{\Gamma}}_j$$

Where; $\hat{\mathbf{M}}_j = \mathbf{M}_j - \mathbf{K}_j\mathbf{G}_j^T\mathbf{M}_j$

$$\mathbf{K}_j = \mathbf{M}_j\mathbf{G}_j(\mathbf{G}_j^T\mathbf{M}_j\mathbf{G}_j)^{-1}$$

$$\hat{\boldsymbol{\Gamma}}_j = \boldsymbol{\Gamma}_j^a - \mathbf{K}_j\mathbf{G}_j^T\boldsymbol{\Gamma}_j^a$$

$$\boldsymbol{\Gamma}_j^a = \boldsymbol{\Gamma}_T + \mathbf{M}_j\boldsymbol{\Lambda}_j$$

B. Non-Terminal Body Recursive Dynamics

Forces acting on a non-terminal link ***j***, in the $(j - 1)^{th}$ body frame

$$\mathbf{R}_{j-1} - \left(\mathbf{T}_{j-1}^j\right)^T\mathbf{R}_j + \mathbf{T}_I^{j-1}(\mathbf{F}_{Dj} + \mathbf{W}_j) = m_j\left(\mathbf{T}_{j-1}^j\right)^T\mathbf{a}_j^m$$

Similarly, summing moments about the connection joint c_{j-1} for the '***j***'[th] link, in the j^{th} frame,

$$\mathbf{r}_j^m \times \mathbf{T}_I^j(\mathbf{F}_{Dj} + \mathbf{W}_j) - \mathbf{r}_j^c \times \mathbf{R}_j + \mathbf{T}_{j-1}^j\mathbf{L}_{j-1} - \mathbf{L}_j = (\mathbf{I}_j\boldsymbol{\alpha}_{j/I} + \boldsymbol{\omega}_{j/I} \times \mathbf{I}_j\boldsymbol{\omega}_{j/I}) + \mathbf{r}_j^m \times m_j\mathbf{a}_j^m$$

The two equations are assembled into matrix form, similar to that of the terminal link. The '**i**' component of the moment equation vanishes and the matrix is reduced to a 5 × 1 system. For a non-terminal link it is expressed as follows:

$$\mathbf{F}_j = \mathbf{M}_j\dot{\mathbf{v}}_j + \boldsymbol{\Gamma}_j + \boldsymbol{D}_{j+1}^T\mathbf{F}_{j+1}$$

Where

$$\boldsymbol{\Gamma}_j = \begin{bmatrix} -\hat{\mathbf{S}}_j^m\mathbf{T}_I^j(\mathbf{F}_{Dj} + \mathbf{W}_j) - \hat{\mathbf{T}}_{j-1}^j\tilde{\mathbf{L}}_{j-1} + \tilde{\mathbf{L}}_j \\ m_j\left(\mathbf{T}_{j-1}^j\right)^T\left(\boldsymbol{\omega}_{J/I} \times (\boldsymbol{\omega}_{J/I} \times \mathbf{r}_j^m)\right) - \mathbf{T}_I^{j-1}(\mathbf{F}_{Dj} + \mathbf{W}_j) \end{bmatrix}$$

As seen in the above equation, the force vector for the 'j[th]' body is coupled to the force vector from the previous link by the term $\boldsymbol{D}_{j+1}^T\mathbf{F}_{j+1}$. The force vector for any non-terminal link can be expressed similarly to the force vector of the terminal link where it depends on its forces and the parent body's joint accelerations. Substituting the terminal link force vector,

$$\mathbf{F}_j = \widetilde{\mathbf{M}}_j\dot{\mathbf{v}}_j + \tilde{\boldsymbol{\Gamma}}_j$$

$$\widetilde{\mathbf{M}}_j = \mathbf{M}_j + \mathbf{D}_{j+1}^T\widetilde{\mathbf{M}}_{j+1}\mathbf{D}_{j+1}$$

$$\tilde{\boldsymbol{\Gamma}}_j = \boldsymbol{\Gamma}_j + \mathbf{D}_{j+1}^T\hat{\boldsymbol{\Gamma}}_{j+1}$$

Again $\mathbf{G}_j^T\mathbf{F}_j = 0$; thus, premultiplying with $\mathbf{G}_j^T$ and solving for $\dot{\boldsymbol{\omega}}_j$ gives

$$\dot{\boldsymbol{\omega}}_j = -\left(\mathbf{G}_j^T\tilde{\mathbf{M}}_j\mathbf{G}_j\right)^{-1}\mathbf{G}_j^T\left(\tilde{\mathbf{M}}_j\mathbf{D}_j\dot{\mathbf{v}}_{j-1} + \boldsymbol{\Gamma}_j^a\right)$$

Where $\boldsymbol{\Gamma}_j^a = \tilde{\boldsymbol{\Gamma}}_j + \tilde{\mathbf{M}}_j\boldsymbol{\Lambda}_j$

Substituting $\dot{\boldsymbol{\omega}}_j$ in the force vector results in the final expression of $\mathbf{F}_j$:

$$\mathbf{F}_j = \hat{\mathbf{M}}_j\mathbf{D}_j\dot{\mathbf{v}}_{j-1} + \hat{\boldsymbol{\Gamma}}_j$$

Where; $\hat{\mathbf{M}}_j = \tilde{\mathbf{M}}_j - \mathbf{K}_j\mathbf{G}_j^T\tilde{\mathbf{M}}_j$

$$\mathbf{K}_j = \tilde{\mathbf{M}}_j\mathbf{G}_j\left(\mathbf{G}_j^T\tilde{\mathbf{M}}_j\mathbf{G}_j\right)^{-1}$$

$$\hat{\boldsymbol{\Gamma}}_j = \tilde{\boldsymbol{\Gamma}}_j + \tilde{\mathbf{M}}_j\boldsymbol{\Lambda}_j - \mathbf{K}_j\mathbf{G}_j^T\boldsymbol{\Gamma}_j^a$$

C. Damping Moment

A damping moment is assumed to exist in each joint. Joint damping has been modeled as viscous damping, proportional to the bending rate between two successive links. Geometrically, this is the relative angular velocity of two links only in the plane they form, i.e. damping comes only from the relative link bending and not the twist.

$$\mathbf{L}_j = -C_s l_j \boldsymbol{\omega}_{j+1/j}$$

Where C_s is the total damping coefficient, $\boldsymbol{\omega}_{j+1/j}$ is the relative angular velocity of two links

5. RECURSIVE SOLUTION

Tether Force ($\mathbf{F}_T$) is calculated from aerostat dynamics. The recursive solution begins with a backward pass through the tether system starting at the terminal link. After calculating $\mathbf{F}_T$, the force vector, $\mathbf{F}_j$ for the terminal link ($j = N$). Formation of force vectors for all non-terminal links then follows for $j = (N - 1)$ to 1. Upon reaching the root link (j = 1), the acceleration vector $\dot{\mathbf{v}}_1$ becomes solvable. Since the root link is attached to the ground, $\mathbf{a}_0^c$ is zero and the solution to $\tilde{\boldsymbol{\alpha}}_{1/I}$ only requires the inversion of a 2 × 2 matrix. Therefore, the solution to $\dot{\mathbf{v}}_1$ is found at the end of the 'backward pass'. Once the acceleration vector, $\dot{\mathbf{v}}_1$, for the root link is known, a forward pass is used to find the angular acceleration vector, $\dot{\boldsymbol{\omega}}_j$, and the acceleration vector, $\dot{\mathbf{v}}_j$, for j = 2 to $N - 1$ then for $j = N$. Completion of the 'forward pass' results in the solution to the N angular accelerations, $\tilde{\boldsymbol{\alpha}}_{j/I}$, for $j = 1$ to N.

6. WIND DISTURBANCES

The aerostat is initially directly above the ground connection with no wind and tether vertical. Orientation of the aerostat is initially facing in the opposite direction of $\mathbf{i}_I$, with ψ_B being π. Wind conditions for the simulation are such that the wind is increased from 0 to 10 m/s over a 10 s interval, with a direction of 15 deg. Aerostat, Visco-elastic, and recursive tether differential equations are numerically integrated.

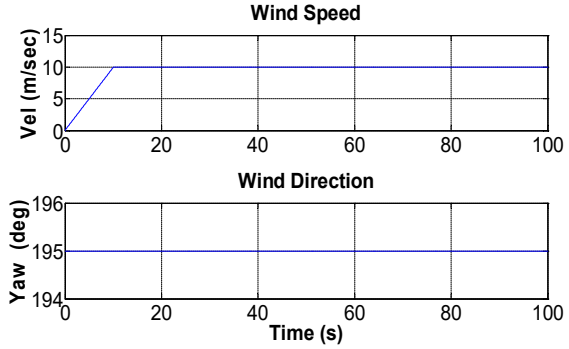

Figure 4: Wind Disturbances

7. RESULTS

Figure 5 shows the horizontal vs vertical displacement response of the system. Figure 6 presents the horizontal plane response of the system. Figure 7 presents the attitude and attitude rates response of the system. Figure 8 presents the tether tension against the time.

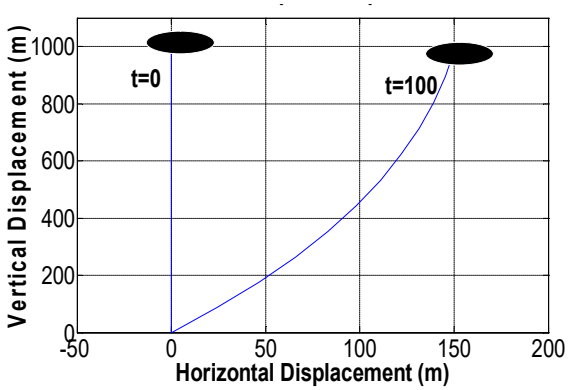

Figure 5: Vertical Plane Response

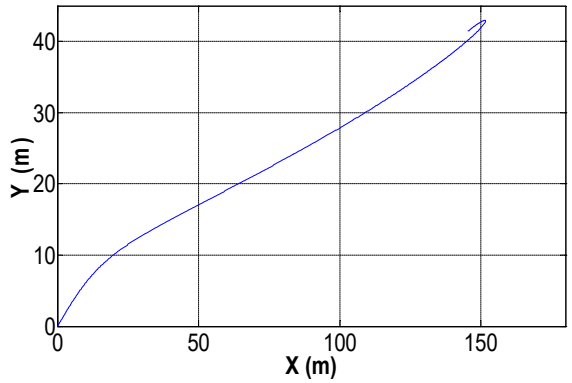

Figure 6: Horizontal Plane Response

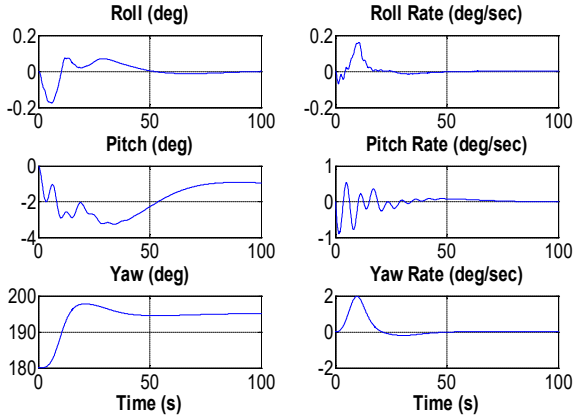

Figure 7: Attitude and Attitude rates

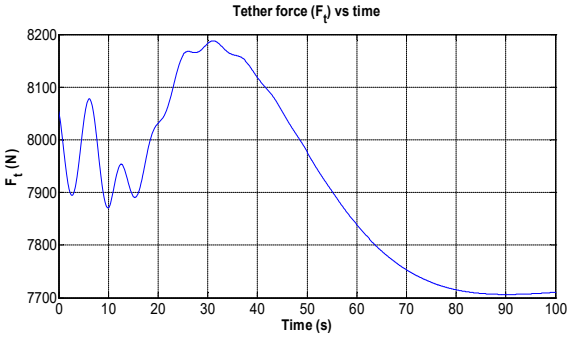

Figure 8: Tether Tension

8. CONCLUSIONS

The results presented for the wind disturbances considered demonstrate the dynamic stability of the system.

The aerostat stabilizes itself at 195^0 yaw angle. This was the expected response of the system, since the wind is at 195^0 direction, hence the tendency of the aerostat should be to rotate about its Confluence Point and stabilize itself in the wind direction with the nose of the balloon pointing into the wind.

Also, the aerostat stabilizes at 0^0 roll, which was the desired performance.

Also, the pitch angle is -1.2^0, which is verified from Static Stability Analysis for 10 m/s wind disturbance. Thus, dynamic stability in pitch is also demonstrated through the simulations.

Acknowledgment

We express our sincere thanks to Director, ADRDE for giving us an opportunity to work on Dynamic Modeling of Aerostat with Tether. We sincerely express our gratitude to Prof A K Ghosh, Department of Aerospace Engineering, IIT Kanpur for his valuable guidance throughout the work. We are also thankful to Sh Amitabha Pal, Sc F, ADRDE, Agra for his valuable comments and suggestions. In the end, we are also thankful to all the members who have directly or indirectly supported or contributed to our present work.

REFERENCES

1. Gabriel A. Khoury and J. David Gillet, 'Airship Technology', 2005.
2. Ajit Kumar, Puneet Gupta and Sudhir Gupta, 'Dynamic Stability Analysis of Aerostat 2000 cum size', ADRDE Report, 2009.
3. Brad Hembree, and Nathan Slegers, 'Tethered Aerostat Modeling using an Efficient Recursive Rigid-Body Dynamics Approach', Journal of Aircraft, Vol. 48, No. 2, March-April, 2011.

1. A Sharma:

Mr. Anuj Sharma did his B. Tech in Aerospace Engineering from IIT Kanpur in 2009. He is currently working as Scientist C at ADRDE (DRDO), Agra on Lighter than Air Technology – Aerostat, in the design, fabrication and testing of the aerostat.

2. A Kumar:

Mr Ajit Kumar did his B. Tech in Mechanical Engineering from BIT Sindri in 2003 and M. Tech in Aerospace Engineering from IISc Bangalore in 2005. Currently he is pursuing PhD in Aerospace Engineering from IIT Kanpur. Presently he is Scientist 'D' in ADRDE (DRDO) Agra and mainly working in the area of aerostat envelope design, structural and dynamic analysis of aerostat envelope.

3. P Gupta:

Mr. Puneet Gupta obtained his Master of Engineering Degree in Space Engg. & Rocketry with specialization in Aerodynamics from Birla Institute of Technology, Mesra, Ranchi in 2005. He is currently working as Scientist D at ADRDE (DRDO), Agra. His main area of work is design, fabrication and testing of various classes of aerostat systems.